NUKLEONIKA 2016;61(2):103–108
doi: 10.1515/nuka-2016-0018

ORIGINAL PAPER

DE GRUYTER
OPEN

Nanostructured targets for TNSA laser ion acceleration

Lorenzo Torrisi,
Lucia Calcagno,
Mariapompea Cutroneo,
Jan Badziak,
Marcin Rosinski,
Agnieszka Zaras-Szydlowska,
Alfio Torrisi

Abstract. Nanostructured targets, based on hydrogenated polymers with embedded nanostructures, were prepared as thin micrometric foils for high-intensity laser irradiation in TNSA regime to produce high-ion acceleration. Experiments were performed at the PALS facility, in Prague, by using 1315 nm wavelength, 300 ps pulse duration and an intensity of 10^{16} W/cm^2 and at the IPPLM, in Warsaw, by using 800 nm wavelength, 40 fs pulse duration, and an intensity of 10^{19} W/cm^2. Forward plasma diagnostic mainly uses SiC detectors and ion collectors in time of flight (TOF) configuration. At these intensities, ions can be accelerated at energies above 1 MeV per nucleon. In presence of Au nanoparticles, and/or under particular irradiation conditions, effects of resonant absorption can induce ion acceleration enhancement up to values of the order of 4 MeV per nucleon.

Key words: target normal sheat acceleration (TNSA) • laser ion acceleration • nanostructures • surface plasmon resonance (SPR)

L. Torrisi✉
Department of Physics Sciences – MIFT,
University of Messina,
V. le F. S. d'Alcontres 31, 981 66 S. Agata, Messina, Italy
and INFN-LNS di Catania, Italy,
Tel.: +39 090 6765052, Fax: +39 090 395004,
E-mail: lorenzo.torrisi@unime.it

L. Calcagno
Dipartimento di Fisica e Astronomia,
Università di Catania,
V. S. Sofia 64, I-95123 Catania, Italy

M. Cutroneo
Nuclear Physics Institute ASCR,
250 68 Rez, Czech Republic

J. Badziak, M. Rosinski, A. Zaras-Szydlowska
Institute of Plasma Physics and Laser Microfusion,
23 Hery Str., 01-497 Warsaw, Poland

A. Torrisi
Institute of Optoelectronics,
Military University of Technology,
2 Kaliskiego Str., 00-908 Warsaw, Poland

Received: 17 September 2015
Accepted: 23 October 2015

Introduction

Ion acceleration from laser-generated plasma occurs at different irradiation conditions, but currently the most employed regime is the target normal sheath acceleration (TNSA) in which thin foils are irradiated by focused lasers at intensities, from above 10^{15} W/cm^2 up to about 10^{20} W/cm^2, and ions are generated from the rear side of the foil, in the forward direction [1]. At lower intensities, the regime is known as backward plasma acceleration (BPA) from thick targets, characterized by high ion yields and low ion energy, of the order of tens of keV/charge state [2]. At very high intensities, obtained using fs laser, the regime is known as radiation pressure acceleration (RPA) in which conditions, very thin foils, of the order of 10 nm in thickness, can be converted in nonequilibrium plasma accelerating relativistic electrons and ions in forward direction above 10 MeV per charge state with about monoenergetic ion beam emission [3]. TNSA regime uses foils with a thickness ranging between 1 and 30 microns and generally permits to accelerate ions, in direction normal to the target surface, above 1 MeV per charge state. The parameters of the laser-generated plasma depends strongly on the kind of used laser, enhancing the electron temperature and density with the $I\lambda^2$ factor, where I is the laser intensity and λ the laser wavelength, depending in duration on the laser pulse width, from ns up to fs scale. The electric field developed in the sheath at the rear side of the foil is correlated to the following relation:

(1) $$E_{\mathrm{TNSA}} = \sqrt{\frac{kT_{\mathrm{e}} n_{\mathrm{e}}}{\varepsilon_0}}$$

where kT_{e} is the electron temperature, n_{e} is the electron density of the generated plasma, and ε_0 is the dielectric constant in vacuum [4]. The electron density follows an exponentially decaying in the longitudinal direction normal to the target rear surface related to the Debye length [5]. Within the cloud of hot electrons in the rear surface, the electric field calculated by Eq. (1) is high enough to ionize atoms from the target surface and accelerate them to MeV energies. The acceleration is sensitive to the charge to mass ratio thus protons are accelerated most effectively.

Moreover, the irradiation conditions control the plasma parameters, for example the laser focal point (LFP) is crucial to develop high electric field of ion acceleration in the rear foil so as the use of p-polarized light (P-PL) can be employed to excite plasma waves enhancing the laser absorption in the plasma or not, depending on the incident angle of the laser light.

In this context, the use of nanoparticles and nanostructures in a thin foil may play an important role on the first instants of laser-matter interaction, enhancing the laser absorption coefficient and inducing resonant absorption effects, as already reported in literature [6]. Surface plasmon resonance (SPR) can be induced using metallic nanoparticles at the surface or embedded into the irradiated foil. The nanoparticles in an insulator medium act so as an induced dipole with opposite polarization with respect to the electric field associated with the incident laser light. Thus a disruptive interference absorbs the laser photons. When the laser frequency is equal to the electron oscillation on the metallic nanoparticle surfaces, resonant absorption occurs and high energy is transferred by laser to the matter. In this work, metallic nanoparticles of gold are embedded to polymer foils to be irradiated in TNSA conditions in order to induce SPR effects and enhance the electron temperature and density of the plasma to generate a higher final ion acceleration in forward direction.

Experimental setup

Three different lasers were used in three different laboratories during this experiment. The first was a low-intensity Nd:YAG laser at the Physics Department of Messina University, operating at 1064 nm wavelength, 3 ns pulse width, and 10^{10} W/cm^2 intensity. This laser was employed to produce Au nanoparticles in liquid and to characterize the plasma at a very low temperature and density. The second one was a medium intensity iodine laser at the PALS laboratory in Prague, operating at 1315 nm wavelength, 300 ps pulse width, and 10^{16} W/cm^2 intensity. The pulse contrast (pre-pulses and ASE) was 10^{-7}. This laser was employed for TNSA ion accelerations in the forward direction in order to quantize their enhancement in presence of SPR effects by Au nanoparticles (Au NP). The third one was a very high-intensity laser, a Ti-sapphire, operating at 800 nm, 43 fs pulse width, and 10^{19} W/cm^2 intensity. The pulse contrast (pre-pulses and ASE) was 10^{-8}. This laser was employed to study TNSA ion acceleration at this high intensity when foils with and without Au nanoparticles are irradiated.

Au nanoparticles were produced irradiating a thick gold target placed in a beaker flask containing the xylene (C_8H_{10}), as shown in Fig. 1a.

The irradiation was performed using 10 Hz repetition rate and the solution was characterized measuring the ablated mass in the volume of the used solvent. The ablated mass was measured as mass difference between the pristine and the full irradiated target. The used solution concentration was 9 mg Au in 15 ml xylene, i.e. 600 μg/ml, as reported in a previous article. In the reported experiment, 5 mg polyethylene (PE) powder was added to the gold solution, which was maintained at 150°C in a rotating beaker for 60 minutes. At the end of the thermal mixing, the final solution was deposited upon flat glasses and let to air dry for 24 hours. Successively, the thin polymeric film was peeled from the glass through the water floating method. Polyethylene films without Au nanoparticles were also produced with the same procedure using xylene as a solvent. The films were measured in thickness using in vacuum the energy loss of alpha particles emitted from a ^{241}Am radioactive source. Film thicknesses between 1 and 15 microns were obtained.

The polymeric foils with dimensions of about 6 mm × 6 mm were attached in a metallic target holder composed of many holes, 3 mm in diameter, as shown in Fig. 1b.

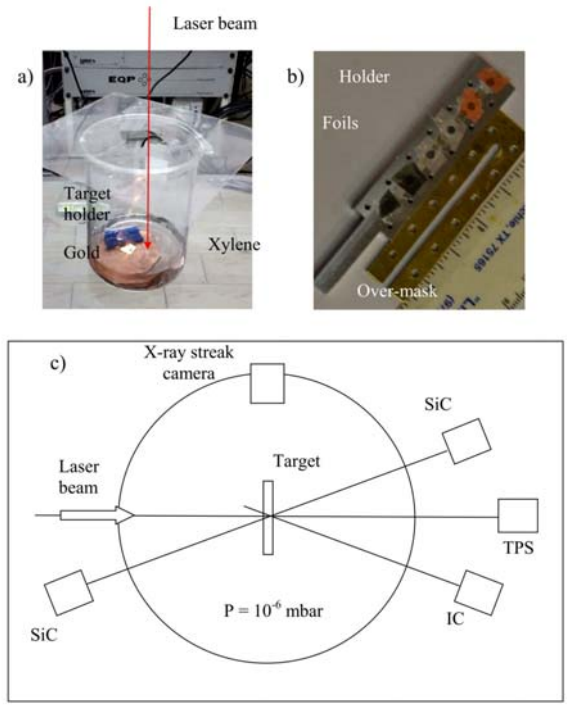

Fig. 1. Setup photo of the apparatus used for the generation of Au NP in liquids: (a) target holder at PALS laboratory for thin foils and TNSA irradiation (b) and scheme of the geometry used during the foil irradiation in vacuum and of the detector positioning (c).

A typical setup of laser irradiation is reported in the sketch of Fig. 1c. Ions are detected in the backward when the low laser intensity is employed, while they are detected in forward when the medium and high laser intensity is used.

The absorption coefficients in the prepared thin foils are enhanced in the presence of Au NP with respect to the pure PE and show resonances at specific wavelength bands depending on the nature, size, and shape of the nanoparticles, and on the nature of the polymer in which they are embedded [7]. The optical characterizations of the produced Au NP show that the spherical shape and the mean diameter of 25 nm produce an absorption resonance at about 550 nm, in the visible region. However, the presence of NP coalescence with the time, producing larger nanostructures with aggregation of 5–10 NP after two to three days at room temperature, shifts the resonance band in the near IR region, around 800–1000 nm, according to literature [8]. Figure 2 shows a measurement of absorbance of the prepared foils with and without Au NP in PE. The Au NP has an average size of about 25 nm (single NP), 100 nm (coalescence of about 4–6 NP), and 1000 nm (coalescence of about 40–60 NP).

The plasma diagnostics is complex but the main detectors consist in ion collectors (IC) that operate as Faraday cups with an electron suppression grid and semiconductor detectors based on SiC-metal Schottky diodes with an energy gap of 3.2 eV and about 10 nA leakage current. Both IC and SiC operate in time of flight configuration at a known distance from the target (60 cm) and at an angle of 30° with respect to the normal to the target surface. At the PALS laboratory, a Thomson parabola spectrometer (TPS) as a diagnostic tool is also used, placed at 0° in the forward direction and a X-ray streak camera (XSC) observing the plasma emission from the top with a resolution time of 1 ns. TPS detects ions, measuring their mass to charge ratios caused by magnetic and electric deflection of a micrometric collimated ion beam emitted from the plasma. XSC coupled to a CCD camera detects the X-ray emission from plasma in a scale of 1 ns exposition time, giving plasma emission images with a lateral resolution of 100 μm. Details on IC, SiC, TPS, and XSC are reported in the previous papers [9, 10].

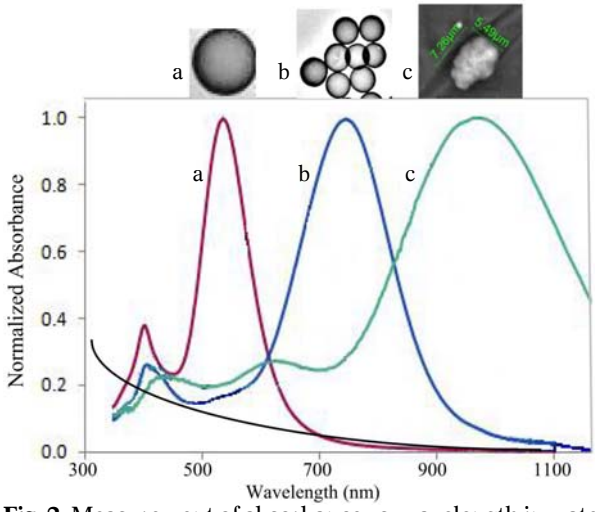

Fig. 2. Measurement of absorbance vs. wavelength in water containing single nanoparticles of Au 25 nm in diameter (a), 4–6 Au nanoparticles in coalescence (b) and micrometric coalescence of Au NP (b).

Experimental results

The study of proton acceleration achieved irradiating polyethylene without and with the Au nanoparticles were conducted using a large range of laser intensity, from 10^9 up to 10^{19} W/cm^2, i.e exploiting ten orders of magnitude.

Figure 3 shows a comparison between two spectra obtained irradiating thick targets (0.5 mm) of pure PE and PE + Au NP through the Nd:YAG laser operating at 10^{10} W/cm^2, 1064 nm wavelength, 3 ns pulse duration, and 0.5 mm spot diameter. The focal position was fixed at about –500 μm from the target surface, i.e. laser is focused 0.5 mm in front of the target surface. TOF spectra were acquired using the IC placed along the normal to the target surface and at 78 cm distance from the target. The maximum proton energy, calculable from the first points of the ion yield, is 92 eV and 143 eV for the pure PE and for the PE containing Au NP, respectively. Moreover, spectra show that the carbon yield increases from about 10 mV up to about 52 mV, demonstrating that at this low laser intensity not only BPA occurs but also that the plasma electron temperature and density are enhanced significantly by the presence of Au NP, inducing SPR absorption effects with the laser light. Of course, the energy of 143 eV calculable for protons is intended as energy per charge state, thus, for example C^{4+} ions have a kinetic energy of about 572 eV.

A better result was obtained by irradiating thin foils with high intensity lasers. Figure 4 shows a comparison between two spectra obtained irradiating pure PE and PE + Au NP using the PALS iodine laser operating at 10^{16} W/cm^2, 1315 nm wavelength, 300 ps pulse duration, and 75 μm spot diameter. In this case, TOF spectra are acquired using the SiC detector placed along the normal to the target surface at 60 cm distance from the target. The maximum

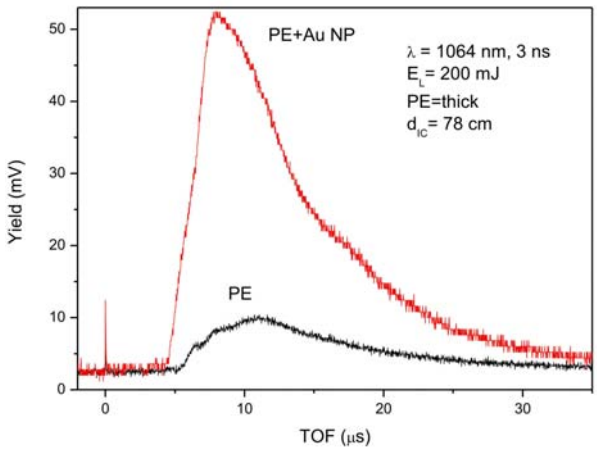

Fig. 3. TOF spectra comparison of ions accelerated at low laser intensity 10^{10} W/cm^2, 3 ns irradiating pure PE and PE + Au NP and detecting in BPA regime.

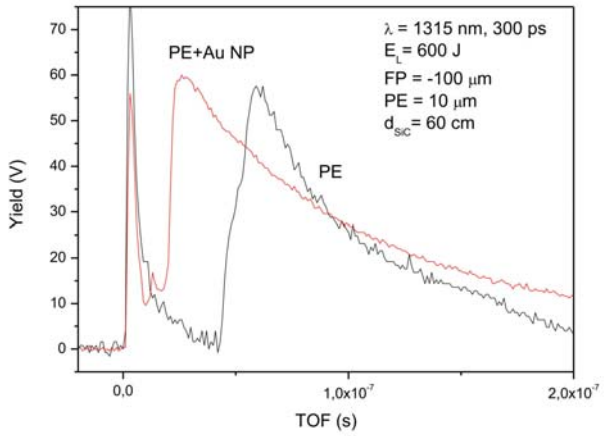

Fig. 4. TOF spectra comparison of ions accelerated at high laser intensity (10^{16} W/cm^2, 300 ps) irradiating pure PE and PE + Au NP and detecting in TNSA regime.

proton energy, calculable from the front of the ion yield, is 1.0 MeV and 4.68 MeV for pure PE and for the polymer with Au NP embedded, respectively. Thus the ion acceleration is strongly increased in the second target because probably SPR absorption effects occur in the laser-matter interaction enhancing the plasma temperature and density. The result of 4.68 MeV for protons is one of the more energetic ion acceleration obtained using this laser at the optimal focal condition of –100 μm, i.e. 100 μm in front of the target surface. From the point of view of the ion yield, it seems that the yield remains approximately the same in the two different plasmas. In this case, all carbon ions are ionized, as demonstrated by the TPS spectra; indeed in the presence of Au NP C^{6+} ions reach a kinetic energy of about 28 MeV.

Figure 5 shows a typical TPS spectrum acquired during the analysis on PE + Au NP. The experimental data are identified thanks to a simulation program that permits to simulate each parabola, giving the value of the magnetic (0.2 T) and electrical (1.4 kV/cm) fields, the geometry of the TPS, and the multichannel plate distance from the electrical field [10]. Parabolas are due to protons, C ions from C^{1+} up to C^{6+}, and Au ions from Au^{1+} up to about Au^{64+}. The high charge states of gold having an ionization potential of 7.1 keV indicate that plasma temperature should be approximately of the same order. The ion energies measured with TPS are in agreement with that measured by SiC.

Figure 6 shows a comparison between two spectra obtained in pure PE and in PE + Au NP foils using the IPPLM laser operating at 10^{19} W/cm^2, 800 nm wavelength, 43 fs pulse duration, and 10 μm spot diameter. TOF spectra are acquired using SiC detector placed along the normal to the target surface (0°) at 80 cm distance. From the TOF relative to the faster ions, it is possible to calculate maximum proton energy of 1.5 and 3.1 MeV for PE and PE + Au NP, respectively. The ion yield decreases in the case of PE + Au NP in contrast with the measurement obtained with the other lasers. However, also in this case, measurements demonstrate that the presence of Au NP enhances significantly the ion acceleration mechanism, but although the used intensity is higher the ion acceleration is lower than the one obtained at the PALS laboratory.

Although in this recent experiment at IPPLM, the laser intensity was three orders of magnitude higher with respect to the experiment at PALS, a lower ion acceleration was obtained. This result is due to the not perfect optimization of the laser parameters, irradiation conditions, and target properties in order to maximize the ion acceleration. Using the fs Ti-sapphire laser, the mechanisms regulating the electric field driving the ion acceleration in TNSA regime are more critical with respect to longer laser pulses, and the contrast, the pedestal duration and intensity, the focal position with respect to the tar-

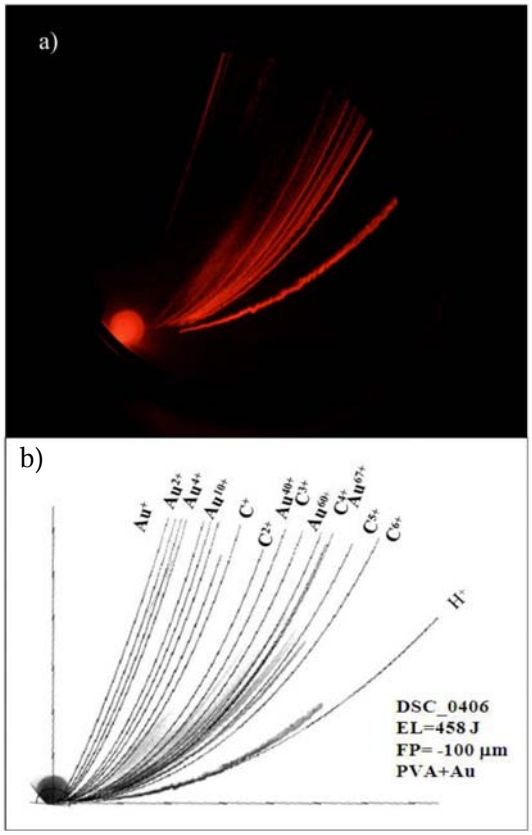

Fig. 5. Typical Thomson parabola spectrum relative to the irradiation of a thin foils of PE + Au NP (a) and identification of the ions, charge states and energy thanks to a simulative program (b).

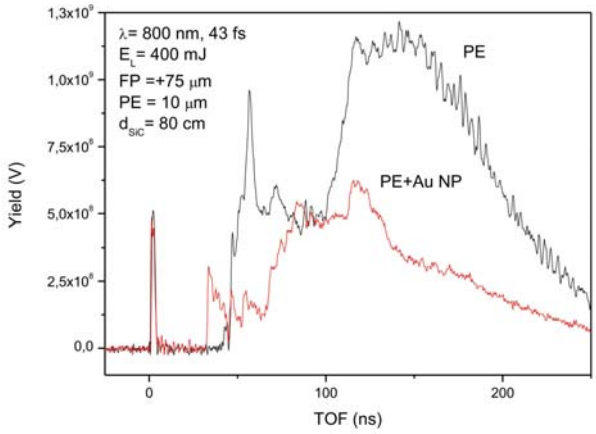

Fig. 6. TOF spectra comparison of ions accelerated at very high laser intensity (10^{19} W/cm^2, 43 fs) irradiating pure PE and PE + Au NP and detecting in TNSA regime.

get surface, the physical target properties, such as roughness, uniformity within the laser focal spot, the target thickness, and SPR absorbance of the NP at the used laser wavelength play important roles that should be optimized accurately in order to maximize the ion acceleration. In the case of PALS experiment, instead, the used advanced targets were optimized in thickness to maximize the ion acceleration, they use Au NP with high absorbance at 1.3 μm wavelength and the focal position of the laser was optimized in order to induce possible self-focusing effects with increment of the ion intensity and consequently of the ion acceleration [11].

Three presented spectra are only indicative of the processes occurring using the same targets but very different laser beams and irradiation conditions. Although many other measurements were performed using the same lasers but different parameters (pulse energy, focal position, incident angle,…), the presented data exhibit the effect that the use of metal nanoparticles may induce enhancing of the laser absorption and the electron density of the target. It is clear the ion acceleration enhancement when metallic NP are enclosed in the polymer but the comparison between different plasmas is not so simple because different setups and irradiation conditions were employed. Many factors influence the plasma temperature, density, duration, ion energy distributions, and charge state distribution and the angular emission of ions and electrons and such factors are very different from them changing the laser intensity and the pulse duration of orders of magnitude. Also the focal position and the focal dimension of the laser pulse play an important role because they may induce self-focusing and filamentation effects in pre--pulse, inducing nonlinear phenomena in plasma that permits to over accelerate ions and electrons [11].

An attempt to compare the obtained results can be given plotting the proton energy for the two targets, without and with Au NP, as a function of the laser intensity, of $I\lambda^2$ parameter, pulse duration, and focal position. These comparisons are reported in the plots of Fig. 7a–c and d, respectively. Such spectra show that the ion acceleration grow with

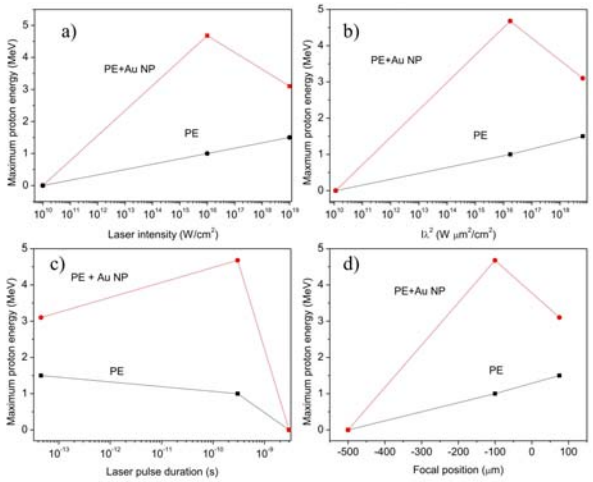

Fig. 7. Plots of experimental data reported as maximum proton energy vs. laser intensity (a), $I\lambda^2$ parameter (b), laser pulse duration, (c) and focal distance (d).

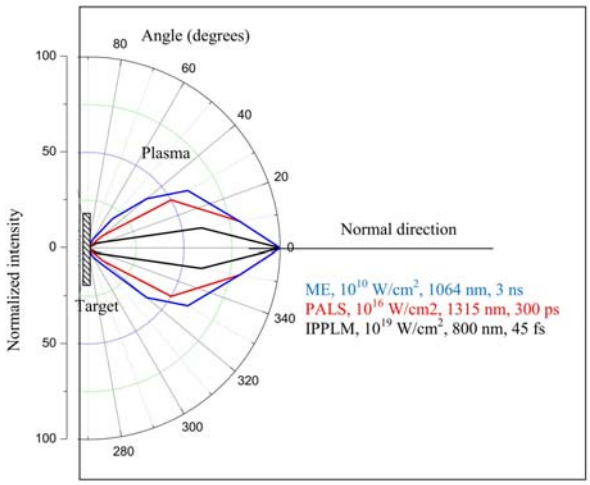

Fig. 8. Comparison of the total ion angular emission from PE for the lasers intensities at 10^{10} (the widest), 10^{16} and 10^{19} (the narrowest) W/cm^2 laser intensity.

the $I\lambda^2$ parameter and depends on the laser pulse duration and focal position. Nonlinear effects are probably due to the use of –100 μm focal position at the PALS that induces self-focusing, as reported in the previous articles [11, 12].

Angular distributions of emitted atoms measured using SiC detectors at different angles with respect to the normal target direction demonstrated that the ion emission is different for the three performed experiments. It is very narrow, of the order of ±10° at very high laser intensity and TNSA regime of 10^{19} W/cm^2 (IPPLM), less directive, and of the order of ±35° at 10^{16} W/cm^2 (PALS) and finally it is large, of about ±55° for BPA plasma ion acceleration at very low intensity of 10^{10} W/cm^2 (ME). Figure 8 shows a comparison between the normalized three total ion distributions obtained irradiating the PE foil with the three different laser pulses.

Discussion and conclusions

Large-scale the physical effects of laser intensities ranging between 10^{10} and 10^{19} W/cm^2 and sub-nanosecond laser pulse duration irradiating polyethylene films, permitting high-energy transfer from a laser beam to the matter, were investigated. At the conditions of the laser 3 ns to 30 fs pulses, many measurements and experiments of laser-matter interaction and plasma characterization should be performed. For this reason, the measurements reported in this article are only preliminary, but an important aspect has been clarified. The use of Au NP embedded inside thin polyethylene foils in all of the described cases seems to enhance the ion acceleration. The explanation of this effect is multiple because it is due to an electron density increment of the target using the highly conductive Au nanostructures arising from the presence of Au nanospheres that show absorption bands at the laser wavelength and in the first instance of the laser-matter interaction enhance the absorption and decrease the reflections and the transmission in the focal point are

also important because may produce preplasma and conditions of self focusing [11, 13].

Despite the expected ion acceleration was higher for fs laser with respect to 300 ps laser, at which the laser intensity is three orders of magnitude higher, in this experiment the maximum ion energy was obtained using the PALS laser and not the IPPLM one. It may depend on many factors due not only to the laser parameters and irradiation conditions but also to the used targets. Using fs lasers, the ion acceleration optimization is more critical with respect to longer pulses, the contrast, the pedestal duration and energy, the focal dimension and position, and the light polarization can modify drastically the plasma properties. Moreover, the dependence of target thickness, composition, and the resonance absorption on the NP size and dimension is different with respect to a laser with a quasi-nanosecond pulse duration, unpolarized, with longer wavelength and higher focal spot, such as that in PALS. In other words, the advanced targets used in this experiment were optimized for 1.3 μm wavelength and 300 ps PALS laser pulses, and not for the fs laser at 800 nm wavelength used at IPPLM.

In the case of fs laser, the relativist electrons accelerated from the laser at the target surface escape at light speed from the target and are not scattered inside due to its low electron density, thus the coupling with the successive escaping ions due to Coulomb explosion is not perfect and the electric field driving the ion acceleration is less pronounced with respect to the experiment at the PALS. Another limiting factor, for example, is represented by the target surface and bulk conditions. The surface roughness may be neglected if the focal spot is of the order of 100 μm but using a spot of 10 μm, comparable with the target roughness, indeed the plasma properties may depend on the morphology of the irradiated target area. Thus, in the case of polymers, due to their preparation roughness of the order of 1–10 μm, not all the laser light has the same focal position from the target surface and a decrement in the plasma electron temperature and density may be induced. Moreover, the Au NP distribution inside the polymeric foil may be not uniform and sometimes agglomerated of Au NP may be present and change locally the target composition if 10 μm focal spot is used.

Of course, by changing the Au NP concentration, the target thickness, the target roughness as well as the laser and the irradiation conditions probably other results would be obtained. In this sense, we are preparing other measurements to explore these interesting aspects with the aim of controlling the plasma properties using advanced targets containing metallic nanostructures and to explain better the ion acceleration for these targets as a function of the laser intensity.

The advantage of obtaining high directivity of the emitted ions using the IPPLM laser, with respect to that at lower intensity, is not negligible because it permits to have high currents of ion emission from plasma with many possible applications of the ion accelerated particles.

Acknowledgments. Work supported by LASERLAB Europe, grant agreement no. 284464, EC's 7th Framework programme.

This work was performed at the University of Messina, Italy, and at IPPLM in Warsaw, Poland.

References

1. Hegelich, B. M., Albright, B. J., Cobble, J., Flippo, K., Letzring, S., Paffett, M., Ruhl, H., Schreiber, J., Schulze, R. K., & Fernández, J. C. (2006). Laser acceleration of quasi-monoenergetic MeV ion beams. *Nature*, *439*(7075), 441–444.
2. Torrisi, L. (2015). Ion acceleration from intense laser generated plasma: methods, diagnostics and possible applications. *Nukleonika*, *60*(2), 207–212.
3. Robinson, A. P. L., Zepf, M., Kar, S., Evans, R. G., & Bellei, C. (2008). Radiation pressure acceleration of thin foils with circularly polarized laser pulses. *New J. Phys*., *10*, 013021.
4. Eliezer, S. (Ed). (2002). *The interaction of high--power lasers with plasmas*. Bristol: Institute of Physics Publishing.
5. Jackel, O., Polz, J., Pfotenhauer, S. M., Schlenvoigt, H. P., Schwooerer, H., & Kaluza, M. C. (2010). All optical measurement of the hot electron sheath driving laser ion acceleration from thin foils. *New J. Phys*., *12*, 103027.
6. Garcia, M. A. (2011). Surface plasmons in metallic nanoparticles: fundamentals and applications. *J. Phys. D-Appl. Phys*., *44*, 283001.
7. Torrisi, L., Cutroneo, M., & Ceccio, G. (2015). Effects of metallic nanoparticles in thin foils for laser ion acceleration. *Phys. Scr.*, *90*(1), 015603.
8. Oldenburg, S. J., Averitt, R. D., Westcott, S. L., & Halas, N. J. (1998). Nanoengineering of optical resonances. *Chem. Phys. Lett*., *288*, 243–247.
9. Cutroneo, M., Musumeci, P., Zimbone, M., Torrisi, L., La Via, F., Margarone, D., Velyhan, A., Ullschmied, J., & Calcagno, L. (2013). High performance SiC detectors for MeV ion beams generated by intense pulsed laser plasmas. *J. Mater. Res*., *28*(1), 87–93.
10. Cutroneo, M., Torrisi, L., Cavallaro, S., Ando', L., & Velyhan, A. (2014). Thomson parabola spectrometer of laser generated plasma at PALS laboratory. *J. Phys. Conf. Series*, *508*, 012020.
11. Torrisi, L., Margarone, D., Laska, L., Krasa, J., Velyhan, A., Pfeifer, M., Ullschmied, J., & Ryc, L. (2008). Self-focusing effect in Au-target induced by high power pulsed laser at PALS. *Laser Part. Beams*, *26*, 379–387.
12. Laska, L., Jungwirth, K., Krasa, J., Krousky, E., Pfeifer, M., Rohlena, K., Ullschmied, J., Badziak, J., Parys, P., Wolowski, J., Gammino, S., Torrisi, L., & Boody, F. P. (2006). Self-focusing in processes of laser generation of highly-charged and high-energy heavy ions. *Laser Part. Beams*, *24*(1), 175–179.
13. Torrisi, L., Calcagno, L., Giulietti, D., Cutroneo, M., Zimbone, M., & Skala, J. (2015). Laser irradiation of advanced targets promoting absorption resonance for ion acceleration in TNSA regime. *Nucl. Instrum. Methods Phys. Res. Sect. B-Beam Interact. Mater. Atoms*, *355*, 221–226.